MOLECULAR IMAGING AND BIOLOGY

Mol Imaging Biol (2019) 21:888–897
DOI: 10.1007/s11307-018-1301-0

Published Online: 20 November 2018

RESEARCH ARTICLE

Quantification of [^{18}F]UCB-H Binding in the Rat Brain: From Kinetic Modelling to Standardised Uptake Value

Maria Elisa Serrano,[1] Mohamed Ali Bahri,[1] Guillaume Becker,[1] Alain Seret,[1] Frédéric Mievis,[2] Fabrice Giacomelli,[2] Christian Lemaire,[1] Eric Salmon,[1] André Luxen,[1] Alain Plenevaux[1]

[1]*GIGA – CRC In Vivo Imaging, University of Liège, Allée du 6 Août, Building B30, Sart Tilman, 4000, Liège, Belgium*
[2]*Nucleis, University of Liège, Allée du 6 Août, Building B30, Sart Tilman, 4000, Liège, Belgium*

Abstract

Purpose: [^{18}F]UCB-H is a specific positron emission tomography (PET) biomarker for the Synaptic Vesicle protein 2A (SV2A), the binding site of the antiepileptic drug levetiracetam. With a view to optimising acquisition time and simplifying data analysis with this radiotracer, we compared two parameters: the distribution volume (Vt) obtained from Logan graphical analysis using a Population-Based Input Function, and the Standardised Uptake Value (SUV).

Procedures: Twelve Sprague Dawley male rats, pre-treated with three different doses of levetiracetam were employed to develop the methodology. Three additional kainic acid (KA) treated rats (temporal lobe epilepsy model) were also used to test the procedure. Image analyses focused on: (i) length of the dynamic acquisition (90 *versus* 60 min); (ii) correlations between Vt and SUV over 20-min consecutive time-frames; (iii) and (iv) evaluation of differences between groups using the Vt and the SUV; and (v) preliminary evaluation of the methodology in the KA epilepsy model.

Results: A large correlation between the Vt issued from 60 to 90-min acquisitions was observed. Further analyses highlighted a large correlation ($r > 0.8$) between the Vt and the SUV. Equivalent differences between groups were detected for both parameters, especially in the 20–40 and 40–60-min time-frames. The same results were also obtained with the epilepsy model.

Conclusions: Our results enable the acquisition setting to be changed from a 90-min dynamic to a 20-min static PET acquisition. According to a better image quality, the 20–40-min time-frame appears optimal. Due to its equivalence to the Vt, the SUV parameter can be considered in order to quantify [^{18}F]UCB-H uptake in the rat brain. This work, therefore, establishes a starting point for the simplification of SV2A *in vivo* quantification with [^{18}F]UCB-H, and represents a step forward to the clinical application of this PET radiotracer.

Key Words: SV2A, PET, [^{18}F]UCB-H, Quantification, Distribution volume, SUV, KASE

Introduction

Positron emission tomography imaging (PET) is able to provide quantitative information about physiological and pathological *in vivo* processes [1–3]. However, to quantify

Correspondence to: Maria Serrano; *e-mail:* meserrano@uliege.be

the results, the PET data must be processed usually by means of kinetic modelling [4–9]. The implementation of this mathematical method requires the use of several blood samples to calculate the arterial input function (IF), which describes the evolution over time of the concentration of the non-metabolised radiotracer in arterial plasma. The necessity of drawing arterial blood samples leads to invasive procedures which hamper any easy application in research and clinical routines [1, 4, 10, 11]. In order to simplify the procedures, alternative approaches have been proposed as, for example, the image-derived IF which allows the measure of the blood tracer concentration directly from dynamic PET images, through the detection of voxels belonging to the aorta, the carotid artery or the heart cavities [12, 13]. Another example is the use of a Population-Based Input Function (PBIF), derived from averaged individual IF obtained from a population [14–18]. However, both options include the use, even when minimal, of blood samples [13]. Other approaches currently employed are the use of a reference tissue with non-existent (or very low) specific uptake [1, 14, 19] or the semi-quantitative Standardised Uptake Value (SUV), which normalise data according to the dose injected and the weight of the individuals [11, 20, 21]. This last parameter, the SUV, appears as an interesting choice in daily clinical and preclinical practices, thanks to the fact that the procedure ensures minimal discomfort to the patient, simple image processing and fast data analysis [1, 10]. Despite the existence of multiple alternatives to quantify PET images, the equivalence between the semi-quantitative parameters, as the SUV, to the quantitative parameters, as the distribution volume (Vt) or the binding potential has seldom been assessed. During the last few years, different studies have focussed on this crucial issue [20], showing in some of them a large correlation between the results expressed in both parameters. Most of these evaluations have been performed in cancerology, using the 2-deoxy-2-[^{18}F]fluoro-D-glucose [21–23]. Currently, the possibility of shortening the acquisition time and simplifying the data analyses for different radiotracers is also being evaluated in neurology [24, 25].

In the present study, we used the [^{18}F]UCB-H, radiotracer which was developed to evaluate the expression of the Synaptic Vesicle protein 2A (SV2A) in the brain [26–29]. This protein is thought to play a key role in the epileptic process. Indeed, current top-of-the-range antiepileptic drugs, such as Levetiracetam (LEV: Keppra®) or Brivaracetam, target this protein to treat the symptoms [30–32]. Furthermore, recent PET studies in healthy volunteers have shown the suitability of this radiotracer as a marker of synaptic density [12, 33]. However, the ubiquitous brain expression of the SV2A protein rules out the use of a reference region to simplify the data analysis [34]. The use of a population-based input function was validated in rats [29]. This interesting approach requires careful validation for the population under investigation. In fact, it has not yet been established with certainty that the input function remains the same for both young and old participants or for healthy and pathological patients.

The aim of this work was to investigate to what extent it would be possible to simplify the procedure for the *in vivo* study of the SV2A proteins with [^{18}F]UCB-H and PET. To this end, we compared two parameters: the distribution volume (Vt), obtained through full kinetic modelling (Logan model) using a Population-Based Input Function [29], and the Standardised Uptake Value.

Materials and Methods

Animals

Five-week-old Sprague Dawley CD rats were obtained from Janvier Laboratories (France) and prior to experimentation, housed in pairs during a two-week period in 12 h:12 h light-dark conditions, while maintaining room temperature at 22 °C, and humidity at approximately 50 %. Standard pellet food and water were provided *ad libitum*.

To develop the methodology, 12 male rats were used. These rats were divided into three groups ($n = 4$ each): LEV 1 mg/kg, LEV 10 mg/kg and SAL. Each animal underwent a pre-treatment consisting an intraperitoneal (IP) injection of either levetiracetam at 1 mg/kg or 10 mg/kg (LEV, Keppra®, UCB Pharma S.A., Belgium) or saline (SAL) 30 min before the PET acquisition. Minimum sample size for the experiment was estimated with G*Power software [35], setting the power level at 0.8 and the alpha level at 0.05. These parameters were set as to detect large effect size ($\eta^2 > 0.5$) differences.

In addition, three supplementary animals were used to perform a preliminary evaluation of the methodology in a temporal lobe epilepsy model (KASE).

Induction of the Temporal Lobe Epilepsy Model

Following the procedure designed by Hellier [36], two of the three animals (KASE) received multiple systemic injections (IP) from 2.5 to 5 mg/kg of kainic acid (KA, kainic acid monohydrate ≥ 99 % (TLC), Sigma Aldrich, USA) every 30 min, until the first convulsive seizure (class 5 on Racine's scale, [37]). The total administered dose was 15 mg/kg for both rats. The third rat (Sham) received multiple systemic injections of saline, instead of KA, serving us as control. These three rats were scanned 12 weeks after the KA/saline administration (chronic phase of epilepsy) [38–40].

Radiochemistry and PET Studies

The enantiomerically pure [^{18}F]UCB-H, referred in [29] as (R)-[^{18}F]UCB-H, was produced through one-step radiolabelling of a pyridyliodonium precursor, in accordance with a reported method [41]. The molar activity reached by this method was 10 Ci/μmol.

The PET acquisition protocol was the same for all the subjects: the [18F]UCB-H (40 ± 3 MBq, 0.55 ml) was administered *via* the caudal vein and, immediately after the radiotracer injection, the PET emission data were recorded in list mode on a Siemens FOCUS 120 microPET (Siemens, Knoxville, TN). Subsequently, a 10-min PET transmission scan was performed in single event acquisition mode, using a Co-57 source. Data were reframed as follows: 6 × 5 s, 6 × 10 s, 3 × 20 s, 5 × 30 s, 5 × 60 s, 8 × 150 s and 6 × 300 s. For each frame, a total of 95 trans-axial slices were obtained using Fourier rebinning (FORE) followed by 2D ramp filtered back projection in a 256 × 256 matrix. The slice thickness was 0.796 mm, and the in-slice pixel size was 0.433 × 0.433 mm^2. The resolution of the system was around 1.5–2.0 mm [42].

Following the PET acquisitions, the rats were transferred into a 9.4T/310 ASR horizontal bore Agilent system and a 72-mm inner diameter volumetric coil (Rapid Biomedical GmbH, Würzburg, Germany). Anatomical magnetic resonance imaging (MRI) of the brain using T2-weighted images were obtained with a fast spin echo multi-slice sequence using the following parameters: TR = 2000 ms, TE = 40 ms, matrix = 256 × 256, FOV = 45 × 45 mm^2, 30 contiguous slices of thickness = 0.80 mm and in-plane pixel size = 0.176 × 0.176 mm^2.

All the imaging procedures were performed under anaesthetic, using 4 % isoflurane in air at a flow rate of 1 l/min for sleep induction and 2 to 2.5 % isoflurane in air at 0.6 l/min for sleep maintenance. The animals remained awake in their cages only between the saline or LEV pre-treatment and the radioactivity administration. Respiration rate and rectal temperature were continuously measured during the PET and MRI scans using a physiological monitoring system. The temperature was maintained at 37 ± 0.5 °C using an air warming system (Minerve, France). During the PET scan, one of the rats pre-treated with LEV 10 mg/kg died, reducing the number of animals of this group to $n = 3$.

Imaging Data Processing

PMOD software (Version 3.6, PMOD Technologies, Zurich, Switzerland) was used to process the imaging data. For each rat, the structural MRI image was manually co-registered with the corresponding PET images and, subsequently, rigid body transformations were applied. The obtained MRI image was then spatially normalised into the PMOD structural MRI image template. Finally, the inversed normalisation parameters were calculated and applied to the PMOD rat brain atlas in order to bring it into the individual PET space. From this atlas, four regions of interest (ROIs) were chosen for the whole experiment due to their significant expression of SV2A: the striatum, the hippocampus, the thalamus and the whole brain.

The SUV was calculated using PMOD from time-activity curves, normalised according to injected dose and animal weight. The Logan plot kinetic modelling (9) was used to obtain Vt at the ROI level, fixing the starting time of the linear section (t*) at 15 min, based on our previous work [27]. PBIF recently published by our laboratory [29] was used to avoid arterial blood sampling during the acquisitions.

Data Analysis

In order to assess the feasibility of shortening the acquisition time and simplifying the data processing, the following steps were considered:

(i) Evaluation of the possibility of shortening the dynamic scan duration: the Vt values for the total 90-min acquisition (Vt-90) were compared with the Vt values issued from the first 60 min of scanning (Vt-60) *via* the Pearson r correlation coefficient and the Bland-Altman method [43, 44], which provides a graphical representation of the differences and possible bias between two sets of data obtained by alternative methods (here, Vt-90 and Vt-60) [45].

(ii) Assessment of the feasibility to perform a static acquisition: the Vt-90 values were compared with the SUV obtained for the various 20-min frames, by means of the Pearson's correlation coefficient. In order to interpret the correlation coefficient strength, we followed the guidelines suggested by Cohen [46]: small correlation: r = ± .10 to ± .29; medium correlation: r = ± .30 to ± .49; large correlation: r = ± .50 to ± 1.

(iii) Analysis of the differences between groups in Vt-90: we used a one-way analysis of variance (ANOVA) followed by a Bonferroni post-hoc tes t in order to detect differences between groups pre-treated with LEV.

(iv) Identification of the optimal time-frame to perform the static acquisition: we performed the same statistical analysis described above, in section (iii), for the 20-min time-frames presenting the largest correlation with the Vt-90 (section (ii)). This analysis will allow us to

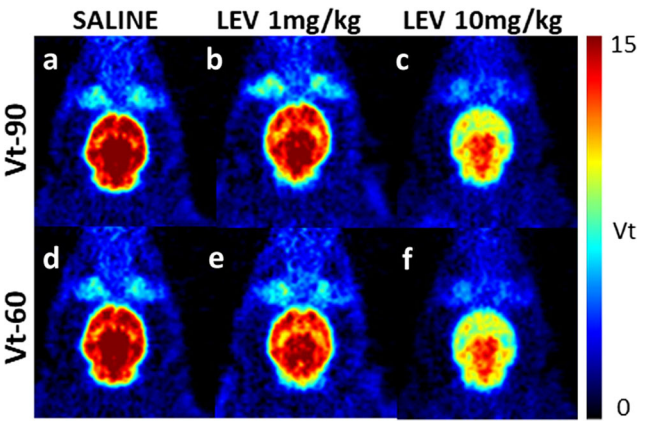

Fig. 1. Representative parametric PET images of [18F]UCB-H binding in rat brain over a 90 min (Vt-90) and b the first 60 min (Vt-60). Rats were pre-treated 30 min before the PET scan with an IP administration with a, d saline; b, e 1 mg/kg LEV; c, f 10 mg/kg LEV.

identify differences between groups in each time-frame. We subsequently compared these results with those observed for the Vt-90 analysis in order to find which of the three time-frames they were equivalent to.

(v) Preliminary evaluation of the methodology in KASE rats: the Vt-60 values were compared with the SUV20-40 and SUV40-60, by means of the Pearson's correlation coefficient.

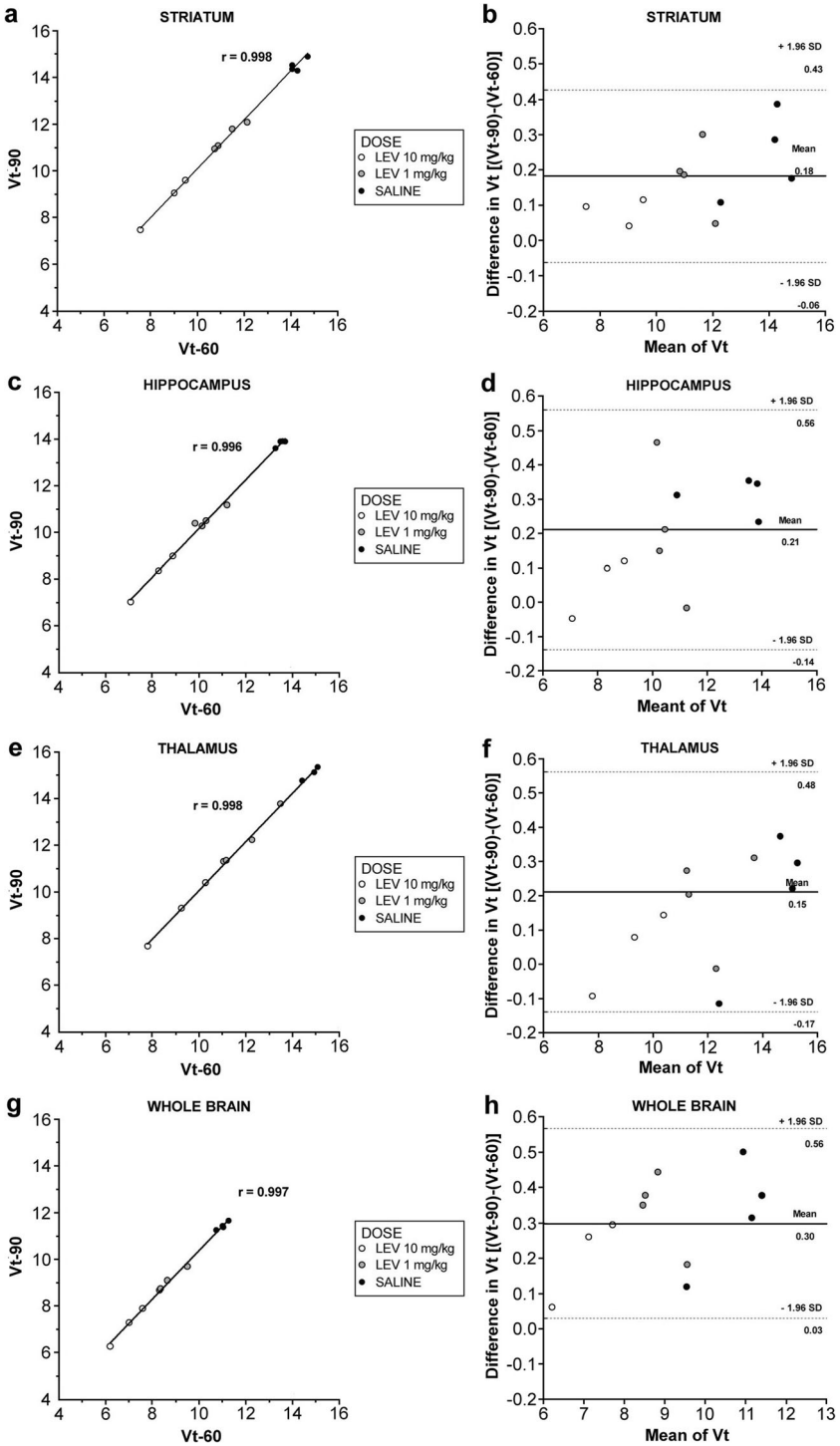

Fig. 2. The scatter plots illustrate the relation between the Vt value obtained for the first 60-min acquisition (Vt-60) and for the whole 90-min acquisition (Vt-90) in **a** striatum, **c** hippocampus, **e** thalamus and **g** whole brain. The value corresponding to the Pearson correlation coefficient is included in bold font. The Bland-Altman plots represent the difference between Vt-90 and Vt-60 values against the mean for the two acquisition schemes, for **b** striatum, **d** hippocampus, **f** thalamus and **h** whole brain. The continuous lines represent the mean of the differences, whereas the dotted lines define the 95 % limits of agreement.

Statistical Analysis

All the statistical analyses were carried out with SPSS (IBM® SPSS® Statistics 24; USA) and the results were given as the mean of SUV or Vt ± the Standard Deviation (SD). The critical level of statistical significance was always set to $p < 0.05$. GraphPad Prism 5 (GraphPad Software, Inc.; USA) was used to graphically represent the results.

Results

Comparison Between Vt-90 and Vt-60

The Vt-90 values, obtained from the total 90-min acquisition (Fig. 1a–c) were compared with the Vt-60 values, issued from the first 60 min of scanning (Fig. 1d–f).

The analyses concerning the equivalence between both parameters highlighted a large correlation ($.996 < r < .998$)

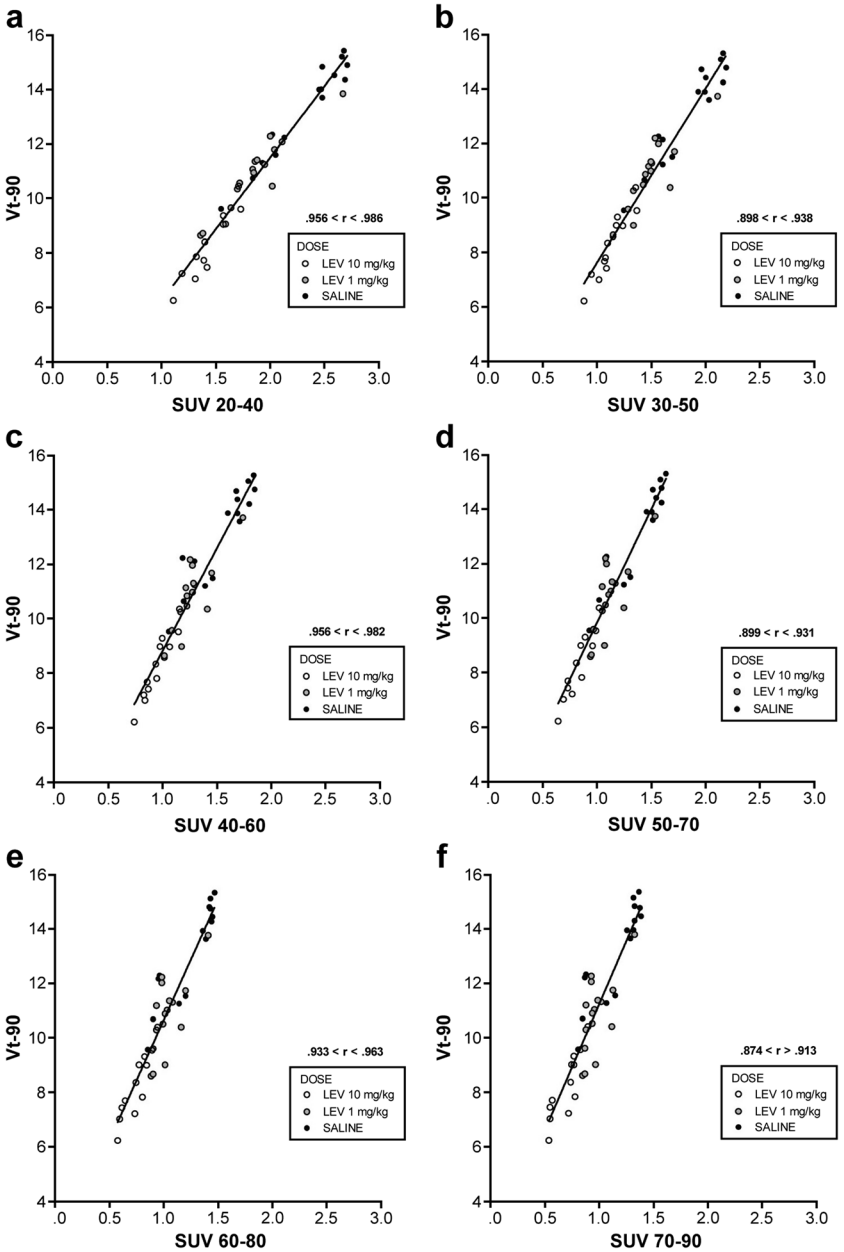

Fig. 3. The scatter plots illustrate the relation between the Vt value for the 90-min acquisition and the SUV parameter for a 10-min sliding window of 20 min duration, equivalent to **a** SUV20-40, **b** SUV30-50, **c** SUV40-60, **d** SUV50-70, **e** SUV 60-80, **f** SUV70-90. The data points correspond to the whole brain and to each of the four regions of interest. The line of best fit for the whole data set is shown in bold, with the range of the Pearson correlation coefficient value obtained when considering each region individually.

which was observed between both values for the four ROIs, considering all rats together ($n = 11$) (Fig. 2a–e & g).

The Bland-Altman analysis (Fig. 2b–f & h) presented no bias between the Vt values obtained for both acquisition times: all the Vt differences [(Vt-90) − (Vt-60)] were within the 95 % limits of agreement (mean ± 1.96*Standard Deviation), and the mean difference was not statistically different from zero ($p > 0.05$).

Correlation Between Vt and SUV

The scatter plots in Fig. 3 illustrate the range of the correlation between the Vt-90 and the SUV computed from the six 20-min frames for the four ROIs. In general, the strength of the correlation considering the three groups together, was large ($r = 0.930 \pm 0.056$), decreasing slightly over time. The largest correlation was detected among Vt-90 and SUV20-40 ($0.956 < r < 0.986$), followed by SUV40-60 ($0.956 < r < 0.982$) and SUV60-80 ($0.933 < r < 0.963$).

Differences Between Groups with Vt-90

We evaluated the differences between groups with Vt, in order to measure the effect of the pre-treatment administered (Fig. 4a). Statistical analysis highlighted a significant effect of the levetiracetam doses used, present in all regions ($p < 0.01$; large effect size: $0.60 < \eta_p^2 < 0.92$). Statistically significant differences were found in the whole brain, the striatum, and the hippocampus between all groups, except between the SAL and the LEV 1 mg/kg groups in the thalamus.

Identification of the Optimal 20-min Time-Frame

The comparison between the results for the Vt-90 and the SUV obtained for three 20-min windows is represented in Fig. 4. Statistically significant differences were equivalent between the dynamic acquisition (Vt-90) and two SUV 20-min frames: SUV20-40 and SUV40-60. The SUV60-80 only allowed to detect the large differences present between SAL and LEV 10 mg/kg groups. These results are consistent with those observed in section (ii), where the largest correlation between the Vt and SUV parameters was observed for the 20–40- and 40–60-min time-frames.

Preliminary Evaluation of the Method in KASE Rats

In Fig. 5, a qualitative comparison of the Sham and one representative KASE rat already highlights differences in [^{18}F]UCB-H binding. We can also appreciate that, as the 20–40-min frame is closer to the injection time, the quality of the image is better than the one reconstructed from 40 to 60 min.

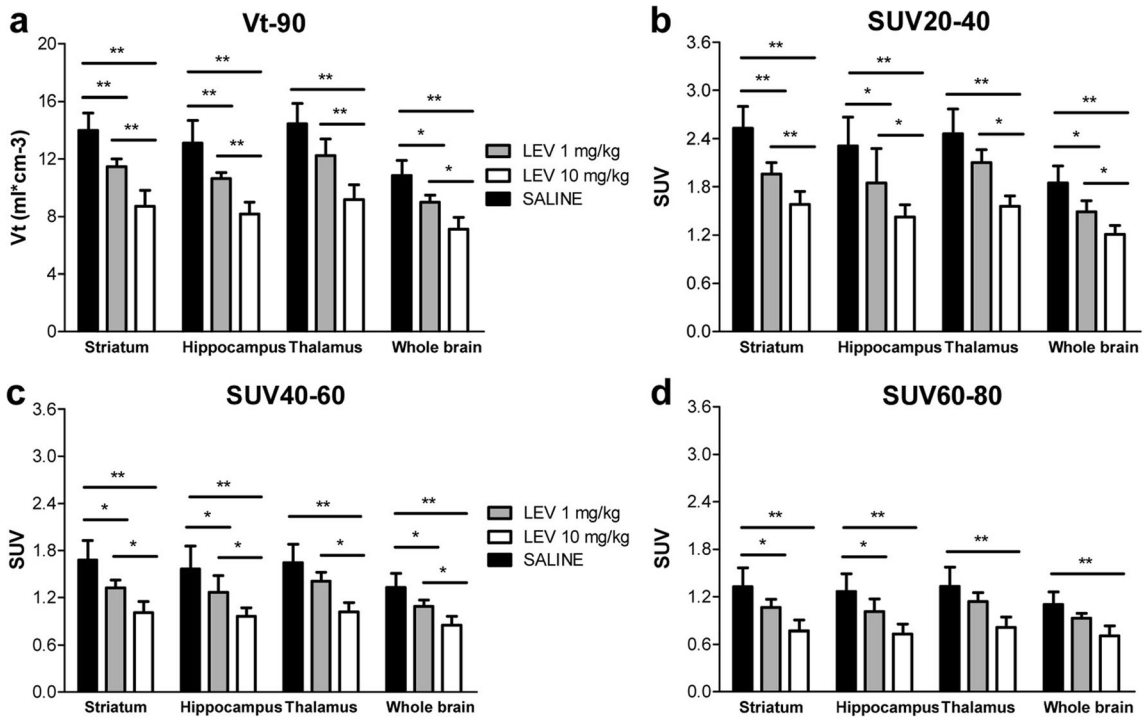

Fig. 4. Differences between groups in **a** Vt-90, **b** SUV 20-40, **c** SUV 40-60 and **d** SUV 60-80 between groups pre-treated with SAL (saline, $n = 4$), LEV 1 mg/kg (n = 4), and LEV 10 mg/kg ($n = 3$). Histograms represent the mean ± SD. *$p < 0.05$; **$p < 0.01$, with one-way ANOVA and Bonferroni post-hoc test.

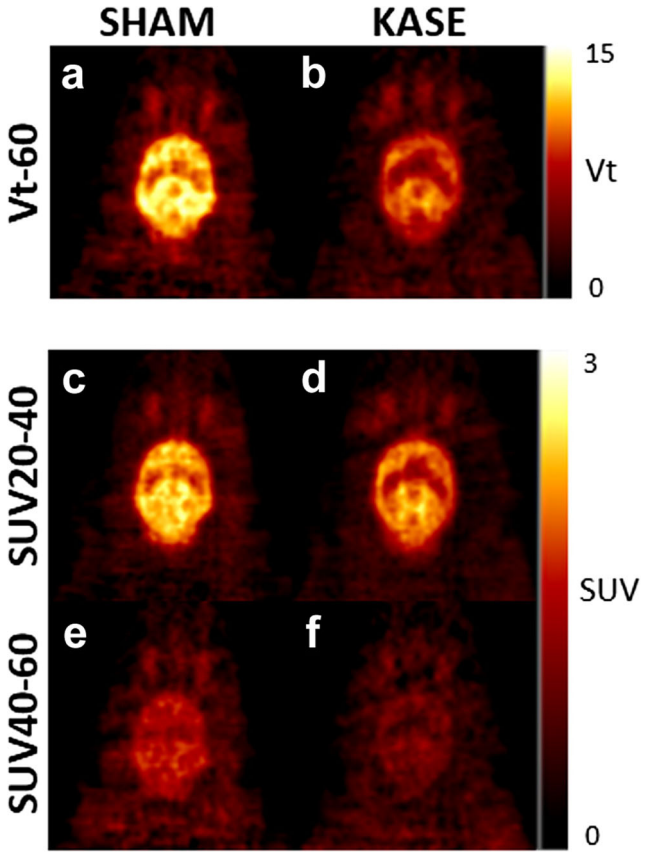

Fig. 5. Illustrative images of [18F]UCB-H binding in rat brain for the first 60 min of scan (Vt-60) for a saline (sham) and b kainic acid–treated (KASE) rats. Images are also presented for 20 to 40 min (SUV20-40) for c sham and d KASE and for 40 to 60 min (SUV40-60) for e sham and f KASE. Animals were treated with multiple systemic (IP) injections of saline (sham) or kainic acid (KASE) and scanned with [18F]UCB-H 12 weeks after (chronic phase of epilepsy).

Differences in the radioactivity uptake for the four ROIs are represented in Fig. 6 a–c: it can be observed that the reduction expressed as percentage of [18F]UCB-H binding in KASE rats, measured with the Vt-60, amounts to 18.4 % ± 3.5 This reduction was around 22.7 ± 8.4 in the case of SUV20-40 and 21.5 ± 8.5 for the SUV40-60.

In Fig. 6d and Fig. 6e, the Vt-60 values were compared for the four ROIs with the SUV20-40 and the SUV40-60, using of the Pearson's correlation coefficient. We can observe that, in both cases, there was a large and significant correlation between the Vt and the SUV parameters.

Discussion

In the present preclinical study, we explored the possibility of optimising acquisition time and data analysis for the recently developed radiotracer [18F]UCB-H. Our goal was twofold: shortening the acquisition time, and validating the use of the SUV to quantify the [18F]UCB-H binding on the brain instead of the Vt. For that purpose, we firstly used rats pre-treated with LEV 1 mg/kg and LEV 10 mg/kg. This pre-treatment will allow us to produce a decrease in the [18F]UCB-H binding around 13.3 % and 25.7 %, respectively [27], similar to those reported in patients with chronic epilepsy and animal models of epilepsy [47]. Subsequently, we applied the methodology to a KASE model, evaluating the [18F]UCB-H binding during the chronic phase.

Our results suggest a large correlation between the Vt measured during the first 60 min and during the whole 90-min acquisition, showing an equivalency of between Vt-60 and Vt-90. Hence, based on these results, we can conclude that it is possible to reduce the time of the dynamic acquisition from 90 to 60 min. This reduction of the acquisition time will facilitate the study with [18F]UCB-H of the pharmacokinetic of new compounds targeting the SV2A protein, but in an optimal period of time and was already applied to obtain the preliminary results with the KASE group.

In addition, in order to facilitate the data analyses and acquisitions, we studied the possibility of performing only static acquisitions with the [18F]UCB-H radiotracer. We started by evaluating the possibility of using the SUV parameter, calculated from 20 min time-frames, instead of the Vt. Statistical results showed a large correlation ($r >$ 0.874) between the Vt and the SUV, particularly from 20 to 40 and from 40 to 60 min. Based on these results, we can conclude that both parameters can be used equally. In previous articles, the strengths and weaknesses of the use of the SUV have been discussed [4, 10, 20]. Briefly, these previous studies showed that, even though the SUV results seem to depend on some factors (such as the quality of the radiotracer administration, or the ROI inaccuracy), when these factors are adequately corrected, the results obtained with the SUV are similar to those obtained through kinetic modelling. In our research, we can also observe equivalent differences between groups with the Vt-90 and the time-frames corresponding to SUV20-40 and SUV40-60. Both parameters can detect statistically significant differences between all the groups. Only in the thalamus, the differences between the saline and LEV 1-mg/kg groups are not statistically significant. Moreover, this group exhibited the highest variability in the measure, which can be explained by the large quantity of SV2A receptors present in this area [48]. An increase in the number of measures might lead to equivalent results for all the ROIs.

With regard to late time-frames, there is still a large correlation between the Vt-90 and the SUV ($r > .5$), but it is weaker than during early time-frames. This decrease in the correlation strength is reflected in a reduced sensitivity to detect differences between groups, as we can see with the SUV60-80 time-frame. A dependency of the SUV on the time interval between injection and scanning has already been highlighted in the literature, explaining these different results [10, 49].

With respect to the most suitable time-frame to perform a static acquisition, we can observe that both, SUV20-40 and

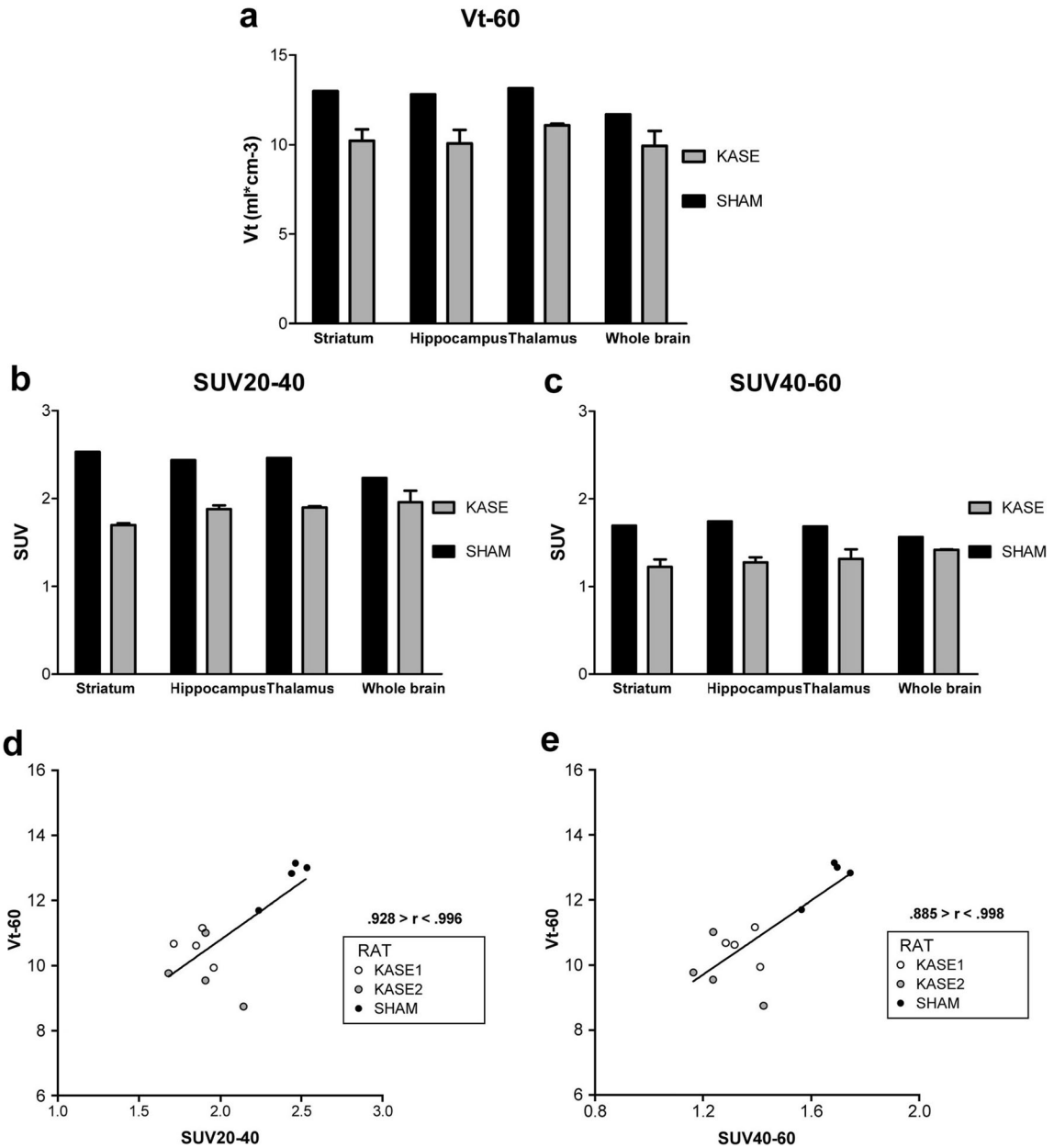

Fig. 6. Preliminary results about differences in [^{18}F]UCB-H binding in KASE rats using Vt-60 and the SUV, and correlation between both parameters. A difference in Vt-60, **b** SUV20-40, **c** SUV40-60 between one rat pre-treated with saline (sham) and two pre-treated with kainic acid (KASE) that were scanned with [^{18}F]UCB-H 12 weeks after the treatment. **d** and **e** illustrate the range of the correlation between the Vt-60 and the SUV20-40 and SUV40-60, respectively.

SUV40-60, seem to produce similar results. However, from a practical standpoint, the quality of the images obtained with SUV20-40 is better, due to the proximity to the injection time. Furthermore, the use of the 20–40-min time-frame will reduce the overall time for the total procedure, making it more suitable than the 40–60-min time-frame.

Finally, the preliminary results obtained with the methodology in the KA epilepsy model highlighted a large correlation between the Vt and the SUV in the case of the [^{18}F]UCB-H, confirming the equivalence between both parameters. Furthermore, the decrease observed in the radiotracer uptake (around 18.4 % with Vt60 and 22.7 % with SUV20-40) were of the same order of magnitude to those reported in the literature, using *in vitro* techniques [47]. However, these results obtained with the KA epilepsy model are preliminary and should be assessed carefully, since the *in vivo* evaluation of SV2A in the case of epilepsy by means of [^{18}F]UCB-H is a research project on its own.

In summary, our results primarily demonstrated the equivalence between the Vt and the SUV parameters when using the radiotracer [^{18}F]UCB-H. Furthermore, they

emphasised the possibility of shortening the acquisition time from 90 to 60 min (dynamic acquisitions) or to 20 min (static acquisition), in the light of the observed large correlation between the Vt and the SUV parameters.

Given the absence of a region of reference for the quantification of the SV2A PET ligands [33, 34], our findings regarding the feasibility of using the SUV lead to an interesting alternative to quantify the [^{18}F]UCB-H *in vivo* binding with PET in rats. This should greatly simplify the use of this radiotracer in preclinical research and is worthy of careful evaluation when applied to humans.

Conclusions

Previous studies have demonstrated the suitability of [^{18}F]UCB-H as an *in vivo* biomarker of the synaptic density since it targets the SV2A protein. In this study, we aimed to optimise the image acquisition procedure, and the subsequent data analysis. We compared the quantification of the [^{18}F]UCB-H binding in the brain through the use of the Standardised Uptake Value (SUV) instead of the quantitative volume of distribution (Vt). Due to the large correlation between the results obtained with the Vt value extracted from dynamic images and the SUV calculated from 20 to 40 min or from 40 to 60 min on simple static images, we highlighted the possibility of shortening the acquisition time from a 90-min dynamic acquisition to an easily accessible 20-min static acquisition and to use the SUV parameter, preferably in a 20–40-min time-frame. These results are worthy of careful evaluation when applied to humans and open the door to a major simplification of data acquisition and analyses for the *in vivo* evaluation of the SV2A proteins with [^{18}F]UCB-H.

Acknowledgments. We would like to thank Miguel Manuel de Villena for the English revision of the manuscript. The authors are grateful to the Nucleis ULiège spin-off technicians for their help producing [^{18}F]UCB-H.

Funding Information. This work was funded by University of Liège grant 13/17-07 and UCB BioPharma as partners. MES is supported by ULiege ARC 13/17 07 grant. AP is research director from FRS-FNRS Belgium.

Compliance with Ethical Standards

Conflict of Interest Statement

The authors declare that they have no conflict of interest.

Ethical Approval

All animal experiments were performed according to the Helsinki declaration and conducted in accordance with the European guidelines for care of laboratory animals (2010/63/EU). All procedures were reviewed and approved by the Institutional Animal Care and Use Ethics Committee of the University of Liege, Belgium.

References

1. Heurling K, Leuzy A, Jonasson M, Frick A, Zimmer ER, Nordberg A, Lubberink M (2017) Quantitative positron emission tomography in brain research. Brain Res 1670:220–234
2. Maria Moresco R, Messa C, Lucignani G, Rizzo G G, Todde S, Carla Gilardi M, Grimaldi A, Fazio F (2001) PET in psychopharmacology. Pharmacol Res 44:151–159
3. Vāvere AL, Scott PJH (2017) Clinical applications of small-molecule PET radiotracers: current progress and future outlook. Semin Nucl Med 47:429–453
4. Acton PD, Zhuang H, Alavi A (2004) Quantification in PET. Radiol Clin N Am 42:1055–1062 viii
5. Cunningham VJ, Gunn RN, Matthews JC (2004) Quantification in positron emission tomography for research in pharmacology and drug development. Nucl Med Commun 25:643–646
6. Fang Y-H, Kao T, Liu R-S, Wu L-C (2004) Estimating the input function non-invasively for FDG-PET quantification with multiple linear regression analysis: simulation and verification with in vivo data. Eur J Nucl Med Mol Imaging 31:692–702
7. Li F, Joergensen JT, Hansen AE, Kjaer A (2014) Kinetic modeling in PET imaging of hypoxia. Am J Nucl Med Mol Imaging 4:490–506
8. Logan J, Fowler JS, Volkow ND, Wolf AP, Dewey SL, Schlyer DJ, MacGregor RR, Hitzemann R, Bendriem B, Gatley SJ, Christman DR (1990) Graphical analysis of reversible radioligand binding from time-activity measurements applied to [N-11C-methyl]-(−)-cocaine PET studies in human subjects. J Cereb Blood Flow Metab 10:740–747
9. Varga J, Szabo Z (2002) Modified regression model for the Logan plot. J Cereb Blood Flow Metab 22:240–244
10. Tomasi G, Turkheimer F, Aboagye E (2012) Importance of quantification for the analysis of PET data in oncology: review of current methods and trends for the future. Mol Imaging Biol 14:131–146
11. Kinahan PE, Fletcher JW (2010) Positron emission tomography-computed tomography standardized uptake values in clinical practice and assessing response to therapy. Semin Ultrasound CT MR 31:496–505
12. Bahri MA, Plenevaux A, Aerts J, Bastin C, Becker G, Mercier J, Valade A, Buchanan T, Mestdagh N, Ledoux D, Seret A, Luxen A, Salmon E (2017) Measuring brain synaptic vesicle protein 2A with positron emission tomography and [^{18}F]UCB-H. TRCI 3:481–486
13. Zanotti-Fregonara P, Chen K, Liow J-S, Fujita M, Innis RB (2011) Image-derived input function for brain PET studies: many challenges and few opportunities. J Cereb Blood Flow Metab 31:1986–1998
14. Rissanen E, Tuisku J, Luoto P, Arponen E, Johansson J, Oikonen V, Parkkola R, Airas L, Rinne JO (2015) Automated reference region extraction and population-based input function for brain [^{11}C]TMSX PET image analyses. J Cereb Blood Flow Metab 35:157–165
15. Mabrouk R, Strafella AP, Knezevic D, Ghadery C, Mizrahi R, Gharehgazlou A, Koshimori Y, Houle S, Rusjan P (2017) Feasibility study of TSPO quantification with [^{18}F]FEPPA using population-based input function. PLoS One 12:e0177785
16. Zanotti-Fregonara P, Hirvonen J, Lyoo CH, Zoghbi SS, Rallis-Frutos D, Huestis MA, Morse C, Pike VW, Innis RB (2013) Population-based input function modeling for [^{18}F]FMPEP-d 2, an inverse agonist radioligand for cannabinoid CB1 receptors: validation in clinical studies. PLoS One 8:e60231
17. Zanotti-Fregonara P, Hines CS, Zoghbi SS, Liow JS, Zhang Y, Pike VW, Drevets WC, Mallinger AG, Zarate CA Jr, Fujita M, Innis RB (2012) Population-based input function and image-derived input function for [^{11}C](R)-rolipram PET imaging: methodology, validation and application to the study of major depressive disorder. Neuroimage 63:1532–1541
18. Zanotti-Fregonara P, Maroy R, Peyronneau M-A, Trebossen R, Bottlaender M (2012) Minimally invasive input function for 2-^{18}F-fluoro-A-85380 brain PET studies. Eur J Nucl Med Mol Imaging 39:651–659
19. Zanderigo F, Ogden RT, Parsey RV (2013) Reference region approaches in PET: a comparative study on multiple radioligands. J Cereb Blood Flow Metab 33:888–897
20. Lammertsma AA (2017) Forward to the past: the case for quantitative PET imaging. J Nucl Med 58:1019–1024
21. Lucignani G, Paganelli G, Bombardieri E (2004) The use of standardized uptake values for assessing FDG uptake with PET in oncology: a clinical perspective. Nucl Med Commun 25:651–656
22. Strauss LG, Dimitrakopoulou-Strauss A, Haberkorn U (2003) Shortened PET data acquisition protocol for the quantification of ^{18}F-FDG kinetics. J Nucl Med 44:1933–1939

23. Dimitrakopoulou-Strauss A, Pan L, Strauss LG (2012) Quantitative approaches of dynamic FDG-PET and PET/CT studies (dPET/CT) for the evaluation of oncological patients. Cancer Imaging 12:283–289
24. Lockhart SN, Baker SL, Okamura N, Furukawa K, Ishiki A, Furumoto S, Tashiro M, Yanai K, Arai H, Kudo Y, Harada R, Tomita N, Hiraoka K, Watanuki S, Jagust WJ (2016) Dynamic PET measures of tau accumulation in cognitively normal older adults and Alzheimer's disease patients measured using [18F] THK-5351. PLoS One 11:e0158460
25. Lopes Alves I, Vállez García DV, Parente A, et al. (2017) Parametric imaging of [11C]flumazenil binding in the rat brain. Mol Imaging Biol 1–10
26. Bretin F, Warnock G, Bahri MA, Aerts J, Mestdagh N, Buchanan T, Valade A, Mievis F, Giacomelli F, Lemaire C, Luxen A, Salmon E, Seret A, Plenevaux A (2013) Preclinical radiation dosimetry for the novel SV2A radiotracer [18F]UCB-H. EJNMMI Res 3:35
27. Warnock GI, Aerts J, Bahri MA, Bretin F, Lemaire C, Giacomelli F, Mievis F, Mestdagh N, Buchanan T, Valade A, Mercier J, Wood M, Gillard M, Seret A, Luxen A, Salmon E, Plenevaux A (2014) Evaluation of ^{18}F-UCB-H as a novel PET tracer for synaptic vesicle protein 2A in the brain. J Nucl Med 55:1336–1341
28. Bretin F, Bahri MA, Bernard C, Warnock G, Aerts J, Mestdagh N, Buchanan T, Otoul C, Koestler F, Mievis F, Giacomelli F, Degueldre C, Hustinx R, Luxen A, Seret A, Plenevaux A, Salmon E (2015) Biodistribution and radiation dosimetry for the novel SV2A radiotracer [^{18}F]UCB-H: first-in-human study. Mol Imaging Biol 17:557–564
29. Becker G, Warnier C, Serrano ME, Bahri MA, Mercier J, Lemaire C, Salmon E, Luxen A, Plenevaux A (2017) Pharmacokinetic characterization of [^{18}F]UCB-H PET radiopharmaceutical in the rat brain. Mol Pharm 14:2719–2725
30. Kaminski RM, Gillard M, Klitgaard H (2012) Targeting SV2A for discovery of antiepileptic drugs. In: Jasper's Basic Mechanisms of the Epilepsies
31. Klitgaard H, Verdru P (2007) Levetiracetam: the first SV2A ligand for the treatment of epilepsy. Expert Opin Drug Discovery 2:1537–1545
32. Nicolas J-M, Hannestad J, Holden D, Kervyn S, Nabulsi N, Tytgat D, Huang Y, Chanteux H, Staelens L, Matagne A, Mathy FX, Mercier J, Stockis A, Carson RE, Klitgaard H (2016) Brivaracetam, a selective high-affinity synaptic vesicle protein 2A (SV2A) ligand with preclinical evidence of high brain permeability and fast onset of action. Epilepsia 57:201–209
33. Mercier J, Provins L, Valade A (2017) Discovery and development of SV2A PET tracers: potential for imaging synaptic density and clinical applications. Drug Discov Today Technol 25:45–52
34. Rabiner EIA (2017) Imaging synaptic density: a different look at neurological diseases. J Nucl Med
35. Faul F, Erdfelder E, Lang A-G, Buchner A (2007) G*Power 3: a flexible statistical power analysis program for the social, behavioral, and biomedical sciences. Behav Res Methods 39:175–191
36. Hellier JL, Patrylo PR, Buckmaster PS, Dudek FE (1998) Recurrent spontaneous motor seizures after repeated low-dose systemic treatment with kainate: assessment of a rat model of temporal lobe epilepsy. Epilepsy Res 31:73–84
37. Racine RJ (1972) Modification of seizure activity by electrical stimulation. II. Motor seizure. Electroencephalogr Clin Neurophysiol 32:281–294
38. Gano LB, Liang L-P, Ryan K, Michel CR, Gomez J, Vassilopoulos A, Reisdorph N, Fritz KS, Patel M (2018) Altered mitochondrial acetylation profiles in a kainic acid model of temporal lobe epilepsy. Free Radic Biol Med 123:116–124
39. Bertoglio D, Amhaoul H, Van Eetveldt A et al (2017) Kainic acid-induced post-status epilepticus models of temporal lobe epilepsy with diverging seizure phenotype and neuropathology. Front Neurol 8:588
40. Van Nieuwenhuyse B, Raedt R, Sprengers M et al (2015) The systemic kainic acid rat model of temporal lobe epilepsy: long-term EEG monitoring. Brain Res 1627:1–11
41. Warnier C, Lemaire C, Becker G, Zaragoza G, Giacomelli F, Aerts J, Otabashi M, Bahri MA, Mercier J, Plenevaux A, Luxen A (2016) Enabling efficient positron emission tomography (PET) imaging of synaptic vesicle glycoprotein 2A (SV2A) with a robust and one-step radiosynthesis of a highly potent 18F-labeled ligand ([^{18}F]UCB-H). J Med Chem 59:8955–8966
42. Kim JS, Lee JS, Im KC, Kim SJ, Kim SY, Lee DS, Moon DH (2007) Performance measurement of the microPET focus 120 scanner. J Nucl Med 48:1527–1535
43. Bland JM, Altman DG (1986) Statistical methods for assessing agreement between two methods of clinical measurement. Lancet (London, England) 1:307–310
44. Bland JM, Altman DG (1999) Measuring agreement in method comparison studies. Stat Methods Med Res 8:135–160
45. Ludbrook J (2008) Statistics in biomedical laboratory and clinical science: applications, issues and pitfalls. Med Princ Pract 17:1–13
46. Cohen J (1988) Statistical power analysis for the behavioral sciences, 2nd editio. Lawrence Erlbaum Associates
47. van Vliet EA, Aronica E, Redeker S, Boer K, Gorter JA (2009) Decreased expression of synaptic vesicle protein 2A, the binding site for levetiracetam, during epileptogenesis and chronic epilepsy. Epilepsia 50:422–433
48. Bajjalieh SM, Peterson K, Linial M, Scheller RH (1993) Brain contains two forms of synaptic vesicle protein 2. Proc Natl Acad Sci U S A 90:2150–2154
49. Ziai P, Hayeri MR, Salei A, Salavati A, Houshmand S, Alavi A, Teytelboym OM (2016) Role of optimal quantification of FDG PET imaging in the clinical practice of radiology. RadioGraphics 36:481–496